Iron Coordination of Activated Bleomycin Probed by Q- and X-Band ENDOR: Hyperfine Coupling to Activated ^{17}O Oxygen, ^{14}N, and Exchangeable ^{1}H

Andrei Veselov,[§,†] Hongjiang Sun,[‡] Andrzej Sienkiewicz,[‡,#] Harold Taylor,[§] Richard M. Burger,[⊥] and Charles P. Scholes*[,§]

Contribution from the Departments of Chemistry and Physics, University at Albany, State University of New York, Albany, New York 12222, and Laboratory of Chromosome Biology, Public Health Research Institute, 455 First Avenue, New York, New York 10016

Received June 20, 1994[⊗]

Abstract: We provide initial electron nuclear double resonance (ENDOR) findings on the electronic structure of iron-containing bleomycin and its activated oxygen. Q-Band (34 GHz) ENDOR has resolved hyperfine couplings from the activated ^{17}O oxygen that originates in isotopically enriched $^{17}O_2$ gas. The largest ^{17}O hyperfine coupling, approximately 27 MHz, was best resolved at an intermediate g-value ($g_y = 2.17$), and a smaller hyperfine coupling, approximately 10 MHz, was resolved at the extremal g_z (g_{max}) and g_x (g_{min}) features as well as at g_y. The wider frequency range and anisotropy of ^{17}O ENDOR features from activated oxygen in bleomycin were in marked contrast to the narrow ENDOR feature of the activated oxyferryl oxygen of horseradish peroxidase compound I (Roberts, J. E.; Hoffman, B. M.; Rutter, R.; Hager, L. P. *J. Am. Chem. Soc.* **1981**, *103*, 7654−7656). The implication of this contrast is that the electronic structure of the activated oxygen differs markedly in the two compounds. The agreement between Q-band ENDOR-resolved hyperfine couplings and hyperfine couplings estimated from X-band EPR line broadening at g_x suggests that there is a large hyperfine coupling to only one oxygen. Hydroperoxide has been indicated as an iron ligand for activated bleomycin (Sam, J. W.; Tang, X-J.; Peisach, J. *J. Am. Chem. Soc.* **1994**, *116*, 5250−5256), and strong hyperfine coupling to one oxygen is compatible with end-on ligation of the hydroperoxide. Exchangeable proton ENDOR patterns, well separated at Q-band from ^{14}N and ^{17}O features, had maximal couplings of the order 13 MHz near the g_z axis, as might be expected for protons which are hydrogen bonded to first shell amine nitrogen or oxygen axial ligands. Activated bleomycin and ferric bleomycin (prepared by chelating ferric ion with bleomycin) differed in details of their proton ENDOR. Nitrogen (^{14}N) ENDOR features and hyperfine couplings resembled those of low-spin ferric heme and imidazole nitrogens.

Introduction

When ferrous bleomycin [Fe(II)-BLM] is exposed to O_2, a transient activated form of bleomycin (Act-BLM) appears which embodies the drug's DNA-cleaving activity.[1a−g] Act-BLM induces DNA strand scission through an oxidative pathway thought to involve free radical intermediates.[2a−c] Isotope studies have shown that oxygen originally provided as O_2 is activated and finds its way ultimately to H_2O.[3a] Electrospray mass spectrometry has strongly suggested that activated bleomycin is a ferric hydroperoxide, formally HOO-Fe(III)BLM,[3b] and the magnitude of an oxygen kinetic isotope effect on breakdown of Act-BLM has indicated a rate-limiting O−O bond cleavage.[3c] In DNA scission, transfer of oxygen directly from Act-BLM to DNA does not occur, but Act-BLM can directly transfer oxygen to olefinic substrates.[3d] Thus Act-BLM is not only a DNA-damaging entity but also a possible model for iron-containing enzymes that activate O_2 and incorporate oxygen into substrates.

Although BLM itself has not been crystallized, two-dimensional NMR[4a−c] shows that it has a metal binding domain which provides nitrogen ligands for the iron, a bithiazole domain which relates to DNA binding, and a mannose-gulose sugar domain. Takahashi and co-workers[3e] pointed out that there is "general agreement that the nitrogens of β-aminoalynyl secondary amine, pyrimidine, and imidazole are equatorial ligands to the iron"; they provided evidence that deprotonated amide nitrogen is a fourth ligand while OH^- serves as an axial ligand for Fe(III)-BLM.[3e] Spectroscopy of models for the iron-binding portion of bleomycin indicates a primary amine nitrogen as one

* Author to whom correspondence should be addressed.
‡ Department of Physics, University at Albany.
§ Department of Chemistry, University at Albany.
⊥ Laboratory of Chromosome Biology, Public Health Research Institute.
† On leave of absence from Institute of Chemical Kinetics & Combustion, 630090, Novosibirsk, Russia.
# Present address: Institute of Physics of the Polish Academy of Sciences, Al. Lotnikow 32/46, 02-668, Warsaw, Poland.
⊗ Abstract published in *Advance ACS Abstracts*, June 15, 1995.

(1) (a) Burger, R. M.; Peisach, J.; Blumberg, W. E.; Horwitz, S. B. *J. Biol. Chem.* **1979**, *254*, 10906−10912. (b) Burger, R. M.; Horwitz, S. B.; Peisach, J.; Wittenberg, J. B. *J. Biol. Chem.* **1979**, *254*, 12299−12302. (c) Burger, R. M.; Adler, A. D.; Horwitz, S. B.; Mims, W. B.; Peisach, J. *Biochemistry* **1981**, *20*, 1701−1704. (d) Burger, R. M.; Peisach, J.; Horwitz, S. B. *J. Biol. Chem.* **1981**, *256*, 11636−11644. (e) Burger, R. M.; Kent, T. A.; Horwitz, S. B.; Münck, E.; Peisach, J. *J. Biol. Chem.* **1983**, *258*, 1559−1564. (f) Burger, R. M.; Blanchard, J. S.; Horwitz, S. B.; Peisach, J. *J. Biol. Chem.* **1985**, *260*, 15406−15409. (g) Kuramochi, H.; Takahashi, K.; Takita, T.; Umezawa, H. *J. Antibiot. (Tokyo)* **1981**, *34*, 578−582.

(2) (a) Takeshita, M.; Grollman, A. P. In *Bleomycin: Chemical, Biochemical, and Biological Aspects*; Hecht, S. M., Ed.; Springer-Verlag: New York, 1979; pp 207−221. (b) Stubbe, J.; Kozarich, J. W. *Chem. Rev.* **1987**, *87*, 1107−1136. (c) Sugiyama, H.; Ohmori, K.; Saito, I. *J. Am. Chem. Soc.* **1994**, *116*, 10326−10327.

(3) (a) Barr, J. R.; Van Atta, R. B.; Natrajan, A.; Hecht, S. M.; van der Marel, G. A.; van Boom, J. H. *J. Am. Chem. Soc.* **1990**, *112*, 4058−4060. (b) Sam, J. W.; Tang, X-J.; Peisach, J. *J. Am. Chem. Soc.* **1994**, *116*, 5250−5256. (c) Burger, R. M.; Tian, G.; Drlica, K. *J. Am. Chem. Soc.* **1995**, *117*, 1167−1168. (d) Hecht, S. M. *Acc. Chem. Rec.* **1986**, *19*, 383−391. (e) Takahashi, S.; Sam, J. W.; Peisach, J.; Rousseau, D. L. *J. Am. Chem. Soc.* **1994**, *116*, 4408−4413.

(4) (a) Akkerman, M. A. J.; Neijman, E. W. J. F.; Wijmenga, S. S.; Hilbers, C. W.; Bermel, W. *J. Am. Chem. Soc.* **1990**, *112*, 7462−7474. (b) Wu, W.; Vanderwill, D. E.; Stubbe, J.; Kozarich, J. W.; Turner, C. J. *J. Am. Chem. Soc.* **1994**, *116*, 10843−10844. (c) Manderville, R. A.; Ellena, J. F.; Hecht, S. M. *J. Am. Chem. Soc.* **1994**, *116*, 10851−10852.

0002-7863/95/1517-7508$09.00/0

of the axial ligands.[5a,b] EPR[1a-f] and NMR[4a] have revealed that there is a site open to external axial ligands like CO, NO, or oxygen. The g-values of Act-BLM (2.26, 2.17, 1.94) are those of low-spin ferric iron, and after preparation of Act-BLM with $^{17}O_2$, broadening of EPR features has demonstrated ligation by oxygen(s).[1d] EPR from non-activated ferric bleomycin [Fe(III)-BLM] has shown g-values[1a,d] of (2.45, 2.18, 1.89) such as those of low-spin ferric cytochrome P450.[1e,6] This article shows the suitability of ENDOR for obtaining structural information on BLM and is the start to probing the intimate electronic structure of iron-containing bleomycin both alone and, ultimately, as perturbed by its DNA substrate.

Experimental Section

Materials. To provide a Q-band sample of Fe-BLM consisting overwhelmingly of activated bleomycin, methods of ref 1e were used. The bleomycin source was Bristol-Myers. Act-BLM for Q-band was prepared in a 1:1 water–ethylene glycol glass with 100% $^{16}O_2$ or with isotopically enriched (82.7%) $^{17}O_2$. The final concentration of the 50-μL Q-band Act-BLM sample was 0.5 mM Fe, 0.7 mM BLM, 20 mM HEPES, 2 mM NADH, 0.05 PMS, 50% (v/v) ethylene glycol. To make the sample, 88 μL of aqueous 1.6 mM BLM, 45 mM Na-HEPES, pH 7.8, were equilibrated with 82.7 atom % $^{17}O_2$ (Isotec Chemicals) at 0 °C in a septum-stoppered 1.5 mL tube, and 4 μL each of 100 mM NADH, 25 mM $Fe^{II}(NH_4)_2(SO_4)_2{\cdot}6H_2O$, and 2.5 mM phenazine methosulfate (PMS) were added with mixing at intervals of 15 s, followed by 100 μL of ethylene glycol. The sample was frozen in liquid nitrogen about 1 min after addition of the Fe(II). The rapid passage Act-BLM spectra (provided to the reviewers) showed little contamination with Fe(III)-BLM. A sample of Fe(III)-BLM was prepared by adding 21 μL of 0.1 M $Fe^{III}NH_4(SO_4)_2{\cdot}12H_2O$ to 399 μL of 6.4 mM BLM, followed by 105 μL of 0.2 M Na-HEPES buffer, pH 7.8. This was lyophilized, reconstituted with 1:1 water:ethylene glycol, and frozen for spectroscopy as above to give a sample of 2 mM concentration in Fe(III)-BLM. Samples requiring solvent deuteration were prepared in 99.9% D_2O and 99% perdeuterated ethylene glycol (MSD Isotopes).

Methods. X-Band (9.2 GHz) ENDOR was carried out as described in ref 7. Q-Band (34 GHz) ENDOR measurements were performed with a home-made newly developed, cryogenically tunable Q-band EPR/ENDOR system having 100 KHz field modulation and ENDOR RF provided by wires internal to the EPR cavity. The system uses the ER 051 QG-D Bruker Q-band bridge having a Gunn diode source. For a several-fold increase of ^{14}N and ^{17}O ENDOR signal intensity, noise broadening of the ENDOR RF was used following methods of ref 8. Microwave power settings for the X-band spectrometer had previously been calibrated vs an X-band power meter in combination with a precision attenuator, and Q-band microwave power settings were taken from the attenuator dial of the ER 051 QG-D bridge. In computing peak frequencies and hyperfine couplings, the frequencies of ENDOR features were corrected for shifts in the direction of the sweep. From spectra swept in opposite directions, the average frequency was obtained. For example, in Figure 1 which was experimentally swept from low to high frequency, the peaks are shifted from their average frequency to a higher frequency by about 1.5 MHz.

For EPR spectral simulations, our goal was to fit with a minimal number of adjustable parameters the EPR line broadening. The adjustable parameters were the ^{17}O electron nuclear hyperfine coupling and the number (either 1 or 2) of equivalent ^{17}O nuclei. The fractional ^{17}O enrichment, f (=0.827 for ENDOR samples), would give the following statistical distribution of species: (1) for a single, magnetically coupled oxygen a fraction $(1-f)$ having no ^{17}O and a fraction f having one ^{17}O; (2) for two magnetically equivalent oxygens a fraction $(1-f)^2$ having no ^{17}O, a fraction $2f(1-f)$ having one ^{17}O, and a fraction f^2 having two ^{17}O. In order to eliminate a need for additional line shape parameters, we used the experimental ^{16}O-Act-BLM EPR line shape as the starting point for simulations of ^{17}O-broadened spectra. To simulate a contribution from a species having one ^{17}O, we convoluted the ^{16}O experimental line shape with a (1:1:1:1:1:1) pattern, and to simulate a contribution from a species having two equivalent ^{17}O, we convoluted the ^{16}O experimental line shape with a (1:2:3:4:5:6:5:4:3:2:1) pattern. The theory used to relate the EPR line shape increase in ^{17}O-containing activated bleomycin only depended on determination of one component of hyperfine coupling at the minimal g-value, g_x, and not on an elaborate multiparameter fitting routine.

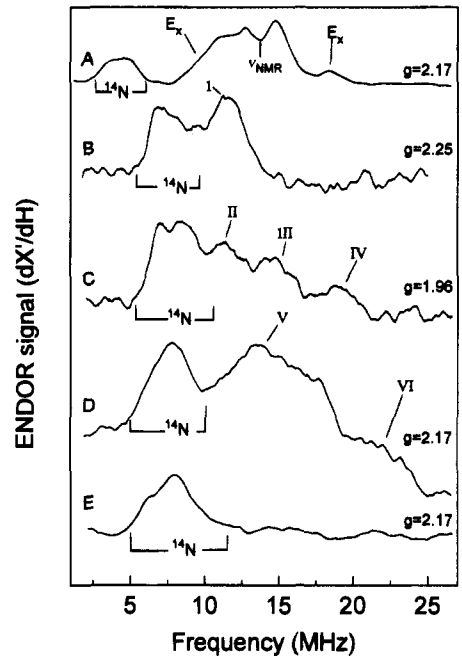

Figure 1. ENDOR spectra over a 1–27-MHz range, all from Act-BLM. All samples shown were in protonated solvent. X-Band Spectrum A was taken at $g_y = 2.17$ from Act-BLM prepared with $^{16}O_2$. Conditions were $T = 4.2$ K, microwave power ~1 μW, magnetic field ~3.01 KG, EPR frequency ~9.17 GHz, RF ~0.5 G p.t.p. (peak-to-peak), frequency sweep rate 2.6 MHz/s, instrumental time constant 0.05 s, 100 KHz field modulation ~1.2 G p.t.p, 10 min of signal averaging. The proton features noted "Ex" were exchangeable. Q-band Spectrum B was taken at $g = 2.25$ from Act-BLM prepared with 82.7% $^{17}O_2$. Conditions were $T = 1.7$ K, microwave power ~3 μW, magnetic field 10.82 KG, EPR frequency 34.0 GHz, RF ~0.5 G p.t.p, frequency sweep rate 2.6 MHz/s, instrumental time constant 0.1 s, 100 KHz field modulation ~1 G p.t.p., 1.9 h signal averaging. Q-band Spectrum C was taken at $g = 1.96$ from Act-BLM prepared with 82.7% $^{17}O_2$. Conditions were the same as for B except that the field was 12.24 KG and 5.4 h of signal averaging were used. Q-Band Spectrum D was taken at $g = 2.17$ from Act-BLM prepared with 82.7% $^{17}O_2$. Conditions were the same as for B except that the field was 11.18 KG and 1.75 h of signal averaging were employed. Q-Band Spectrum E was taken at $g = 2.17$ from Act-BLM prepared with naturally abundant $^{16}O_2$ showing ^{14}N couplings. Conditions were the same as for D except that 1 h of signal averaging was employed. The position of this ^{14}N feature moved by less than 1 MHz over the entire EPR line shape of Act-BLM.

Results and Discussion

X-Band ENDOR Results. At X-band the major ENDOR features from Act-BLM (spectrum 1A) were proton features centered at the free proton frequency, ν_{NMR}, near 13 MHz.[9a] Some of these proton features were exchangeable in deuterated solvent. There were features in the 3–5-MHz region which were similar in appearance and frequency to those of heme and imidazole nitrogen in low-spin ferric heme[7] where nitrogen

(5) (a) Guajardo, R. J.; Hudson, S. E.; Brown, S. J.; Mascharak, P. K. *J. Am. Chem. Soc.* **1993**, *115*, 7971–7977. (b) Guajardo, R. J.; Tan, J. D.; Mascharak, P. K. *Inorg. Chem.* **1994**, *33*, 2838–2840.

(6) LoBrutto, R.; Scholes, C. P.; Wagner, G. C.; Gunsalus, I. C.; Debrunner, P. G. *J. Am. Chem. Soc.* **1980**, *102*, 1167–1170.

(7) Scholes, C. P.; Falkowski, K. M.; Chen, S.; Bank, J. F. *J. Am. Chem. Soc.* **1986**, *108*, 1660–1671.

(8) Hoffman, B. M.; DeRose, V. J.; Ong, J. L.; Davoust, C. E. *J. Magn. Reson.* **1994**, *110*, 52–57.

features observed at X-band centered at $|^1/_2A^N + {}^{14}\nu|$, i.e., in the ν^+ branch.[9b] The coupling, $|A^N|$, of such features was in the 5−6-MHz range. The present features probably represent an overlapping compendium of similar couplings from several of the liganding nitrogens. The corresponding ^{14}N features of spectrum 1E at Q-band peaked at 6.1 ± 0.3 MHz, and since $^{14}\nu$ = 3.4 MHz at Q-band, $|A^N|$ = 5.2 ± 0.3 MHz.

^{17}O ENDOR and EPR Results. Even with solvent deuteration we resolved no features in X-band ENDOR of Act-BLM that we could unambiguously attribute to ^{17}O couplings.[10a-c] The compendium of proton ENDOR features near 13 MHz interfered with ^{17}O resolution.[10d] The fields used for Q-band shift the protons to frequencies >30 MHz.[9a] Spectra 1B, 1C, and 1D, taken at Q-band from Act-BLM prepared with $^{17}O_2$, showed new features attributable to ^{17}O in the 9−23-MHz region. Such features were *not* observed in spectrum 1E from Act-BLM prepared with $^{16}O_2$.

For ^{17}O ENDOR one expects a ν^+ branch of ^{17}O ENDOR features centered at $|^1/_2A^{17} + {}^{17}\nu|$ and a ν^- branch centered at $|^1/_2A^{17} - {}^{17}\nu|$.[11] The ν^+ branch has in other work generally been the more intense.[10b,c] In our work we expected to observe the ν^+ branch because the ν^- branch is weak and falls near 0 MHz.[12] At extremal g-values ($g_z = g_{max}$ or $g_x = g_{min}$) the magnetic field typically picks out a small spread of orientations that are close to the respective **g** tensor direction. Within such orientations well-defined single-crystal-like ENDOR patterns occur that reflect a single effective value of the hyperfine coupling rather than a spread of values arising from a powder pattern.[13a-c] Close to g_z there was indeed a single, relatively narrow, structureless ^{17}O ENDOR feature (spectrum 1B, feature I), with a peak frequency of 9.8 ± 0.3 MHz; its hyperfine coupling was computed as 7.1 ± 0.3 MHz. At g_x (spectrum 1C) there was an ENDOR pattern of at least three features (II, III, IV) at 10 ± 0.6, 13.1 ± 0.6 , and 17.4 ± 0.8 MHz, respectively. The hyperfine coupling of the central feature III was computed as 11.9 ± 0.6 MHz. It is likely that the three-line structural detail of spectrum 1C represents the central part of a quadrupolar pattern with splitting ($3Q$) of ~3.5 MHz and $|Q| \sim 1.2$ MHz.[14ab] Quadrupole couplings have been reported from ^{17}O-hydrogen peroxide which translate into a value of $|Q|$ = 0.8 MHz.[15]

At the intermediate g-value ($g_y = g_{inter}$) the EPR and ENDOR intensities were largest, but at the intermediate g-value numerous orientations may contribute and broad powder ENDOR patterns result.[13a-c] At g_y (spectrum 1D) ENDOR intensity stretched from a broad peak (feature V) at 11.5 ± 0.6 MHz to a shoulder (denoted VI) at 20 ± 1.2 MHz; the hyperfine coupling of feature V was computed as 10.1 ± 0.6 MHz (similar to the hyperfine coupling measured at g_x and g_z) and the hyperfine coupling of the shoulder from feature VI as 27 ± 1.2 MHz.

ENDOR measures ligand hyperfine coupling with considerable resolution but gives less information on the number of identical contributing ligands. Because the EPR absorption line shape depended on hyperfine couplings *and* the number of contributing ligands, EPR line broadening gave information complementary to ENDOR. X-Band EPR line broadenings were observed at g_y and g_x but not at g_z.[1d,16] The g_x feature showed ^{17}O-induced broadening and, unlike the g_y feature, was at an extremal g-value where the complication of many orientations should be less. Experimental EPR traces of the ^{17}O-induced line broadening at g_x for samples having 82.7 atom % enrichment of $^{17}O_2$ are shown in the supporting information (Figure 1-S, A and B). From simulations (Figure 1-S, C and D) at g_x we estimated that a one-oxygen model gave its best fit with a hyperfine coupling of 4.4 G = 12 MHz and a two-equivalent-oxygen model gave an equally good fit with a hyperfine coupling of 3.2 G = 8.7 MHz. Our ENDOR estimate of the hyperfine coupling at g_x was 11.9 MHz. The average coupling for the overall pattern (II, III, IV) is definitely not as small as 8.7 MHz.[14b]

^{17}O Discussion. Act-BLM contains the same number of oxidizing equivalents as compound I of horseradish peroxidase (HRP), i.e., two reducing equivalents are required to discharge Act-BLM to Fe(III)-BLM.[1f,3b] In HRP compound I, one oxidizing equivalent exists as the porphyrin π-cation radical while the other oxidizing equivalent involving the ENDOR-detectable activated oxygen is a S = 1 oxyferryl (Fe^{IV}=O) moiety, spin coupled to the π-cation. The activated oxygen of the oxyferryl moiety, which was the first activated oxygen to be probed by ENDOR, gave a single sharp ENDOR feature lacking quadrupolar structure with hyperfine coupling in the 17−19-MHz range.[16] In contrast, the iron of Act-BLM is in a low-spin ferric state.[1a,d,e] The spectral anisotropy and generally broader ^{17}O ENDOR features of activated oxygen in Act-BLM are markedly unlike those observed by ENDOR of the oxyferryl oxygen of HRP compound I.

The differences in ^{17}O ENDOR spectra taken at g_z, g_y, and g_x were clear evidence for anisotropy in the hyperfine interaction. The smaller hyperfine couplings ($|A_\perp| \sim 10$ MHz) measured at g_x and g_z showed that there is a plane of smaller ^{17}O hyperfine couplings occurring at or near the g_x−g_z plane. It is hard to envision a scenario where the maximal hyperfine coupling also lies in this g_x−g_z plane of small hyperfine

(9) (a) For protons the first-order ENDOR frequency is $\nu^H = |\nu_{NMR} \pm A^H/2|$, where A^H is the electron proton hyperfine coupling. (b) For a ^{14}N I = 1 nucleus the first-order ENDOR frequencies are as follows: the ν^+ branch at $\nu^+ = |^1/_2A^N + {}^{14}\nu \pm Q|$ and the ν^- branch at $\nu^- = |^1/_2A^N - {}^{14}\nu \pm Q|$, where A^N is the ^{14}N hyperfine coupling, $^{14}\nu$ is the nitrogen NMR frequency (~0.9 MHz at 3 KG and 3.4 MHz at 11.2 KG), and Q is the quadrupole coupling.

(10) (a) Werst, M. M.; Kennedy, M. C.; Beinert, H.; Hoffman, B. M. *Biochemistry* **1990**, *29*, 10526−10532. (b) Jin, H.; Turner, I. M.; Nelson, M. J.; Gurbiel, R. J.; Doan, P. E.; Hoffman, B. M. *J. Am. Chem. Soc.* **1993**, *115*, 5290−5292. (c) In several systems reported in refs 10a and 10b the ^{17}O ENDOR features are narrow with resolved quadrupolar structure and stand out even though there are other underlying ENDOR features of other nuclei; this was not the case with ^{17}O-Act-BLM. (d) Werst, M. M.; Davoust, C. E.; Hoffman, B. M. *J. Am. Chem. Soc.* **1991**, *113*, 1533−1538.

(11) First-order ^{17}O ENDOR frequencies for a ^{17}O $I = {}^5/_2$ nucleus are as follows: the ν^+ branch at $|^1/_2A^{17} + {}^{17}\nu|$, $|^1/_2A^{17} + {}^{17}\nu \pm 3Q|$, $|^1/_2A^{17} + {}^{17}\nu \pm 6Q|$ and the ν^- branch at $|^1/_2A^{17} - {}^{17}\nu|$, $|^1/_2A^{17} - {}^{17}\nu \pm 3Q|$, $|^1/_2A^{17} - {}^{17}\nu \pm 6Q|$. A^{17} is the hyperfine coupling, $^{17}\nu$ (6.24 MHz at 10.82 KG, 6.45 MHz at 11.18 KG, and 7.17 MHz at 12.42 KG) is the ^{17}O nuclear Zeeman interaction, and Q is quadrupolar coupling. In terms of the frequently used quadrupole coupling constant, e^2qQ, the quadrupole coupling which we use in our ENDOR expressions is $Q = e^2qQ/[2I(2I-1)h] = e^2qQ/(20h)$.

(12) Had the ν^- branch been in the frequency range 12−15 MHz, we would have predicted a ν^+ branch in the 25−30 MHz range and larger ^{17}O hyperfine couplings that would have led to a much more broadened EPR line width. Neither a 25−30-MHz ENDOR feature nor a broader EPR line width were observed.

(13) (a) Hoffman, B. M.; Martinsen, J.; Venters, R. A. *J. Magn. Reson.* **1984**, *59*, 110−123. (b) Hoffman, B. M.; Venters, R. A.; Martinsen, J. *J. Magn. Reson.* **1985**, *62*, 537−542. (c) Hoffman, B. M.; DeRose, V. J.; Doan, P. E.; Gurbiel, R. J.; Houseman, A. L. P.; Telser, J. In *Biological Magnetic Resonance, Vol. 13: EMR of Paramagnetic Molecules*; Berliner, L. J.; Reuben, J., Eds.; Plenum Press: New York, 1993.

(14) (a) According to ref 11 above, the ν^+ branch for $I = {}^5/_2$ ^{17}O would ideally be expected to have five features, split from each other by the quadrupolar splitting, $3Q$. Within the signal-to-noise of spectrum 1 C at g_x we cannot rule out the possibility of a fourth weak ^{17}O feature near 20 MHz, and a fifth ^{17}O feature which may be obscured under the ^{14}N feature near 7 MHz. (b) If their ENDOR frequencies could be ascribed entirely to hyperfine and nuclear Zeeman interactions exclusive of a quadrupolar contribution, the hyperfine couplings calculated from Features II, III, and IV would respectively be 5.7, 11.9, and 20.5 MHz; the average of these three couplings is 12.4 MHz.

(15) Lumpkin, O.; Dixon, W. T. *J. Chem. Phys.* **1979**, *71*, 3510−3511.

(16) Roberts, J. E.; Hoffman, B. M.; Rutter, R.; Hager, L. P. *J. Am. Chem. Soc.* **1981**, *103*, 7654−7656.

couplings. The maximal hyperfine coupling would occur perpendicular to the g_x-g_z plane, suggesting that $A_{||}$ is near the g_y tensor direction, although without detailed analysis,[13a-c] we cannot say with what precision $A_{||}$ is aligned along g_y. Still, it is significant that the largest ^{17}O hyperfine coupling ($|A_{||}| \sim 27$ MHz) was experimentally measured from the frozen solution EPR pattern at the intermediate g-value of g_y.[17] The difference between $|A_{||}|$ and $|A_\perp|$ is ~17 MHz. The difference between $A_{||}$ and $A_\perp$ for a single unpaired oxygen p electron is 420 MHz.[18] If our $A_{||}$ and $A_\perp$ difference were entirely due to the hyperfine anisotropy of unpaired spin in a $p\pi^*$ orbital, that orbital would contain ~4% of an unpaired electron, and the lobes of the $p\pi^*$ orbital would point along the $A_{||}$ tensor direction. (For the oxyferryl oxygen of HRP compound I the spin density on the ^{17}O arose from a spin-coupled excited state and the amount of unpaired electron spin actually on the oxygen was significant, ~25% in HRP compound I,[16] larger than the above 4%.)

Taylor has related the **g**-tensor for a low-spin ferric ion to the orbital contributions of d_{xy}, d_{xz}, and d_{yz} orbitals.[19] For the g-values of Act-BLM his treatment (eq 5 of ref 19) predicts that the vast majority of spin on the iron be in the d_{yz} orbital; the orbital coefficient of the d_{yz} orbital for Act-BLM is >0.99. The treatment of Taylor does not inherently specify the ligand axes that coincide with x, y, or z directions. However, the transfer of electron spin between metal and activated oxygen would best occur if there is overlap between an oxygen $p\pi^*$ orbital and the d_{yz} orbital. The line of maximum overlap between a spin-containing oxygen $p\pi^*$ orbital and the metal d_{yz} orbital should parallel the direction of maximal ^{17}O hyperfine coupling which is the direction of $A_{||}$ and (here) approximately the direction of g_y.

The agreement between ENDOR-resolved hyperfine couplings and hyperfine couplings estimated from EPR line broadening at g_x is consistent if there is *one* contributing oxygen to the EPR pattern. The single relatively narrow ENDOR feature at g_z is also consistent with coupling to one oxygen.[20] If the iron ligand is hydroperoxide,[3b] it seems unlikely that hydroperoxide would have identical oxygen hyperfine couplings from each of its oxygens if one hydroperoxide oxygen is bound to iron and the other to a proton. A conceivable mode of hydroperoxide ligation would be end-on ligation by the oxygen whose hyperfine coupling we measure by ENDOR. We propose that there could be a smaller hyperfine coupling to the more distant hydroperoxide oxygen that has not yet been measured by ENDOR and might best be measured by ESEEM.

Q-Band Proton ENDOR Results. Proton ENDOR is shown in Figure 2 for Act-BLM and for Fe(III)-BLM as obtained near g_z, g_y, and g_x. Close to the maximal (g_z) g-value proton couplings of the order 13 MHz were observed from protons which were found to be exchangeable (spectra 2A and 2B). With Act-BLM there was a notable additional exchangeable feature with coupling of about 7 MHz. At the intermediate (g_y) g-value

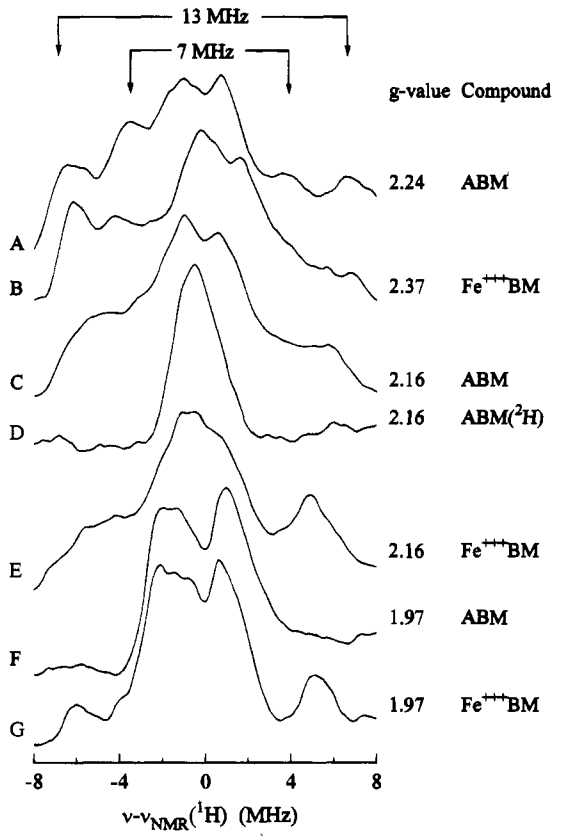

Figure 2. Proton ENDOR spectra obtained at Q-band (34.0 GHz). These spectra were taken at $T = 1.7$ K, with a frequency sweep rate of 1.3 MHz/s, 3 μW microwave power, RF of ~0.5 G p.t.p, 100 KHz field modulation of ~1 G p.t.p., and instrumental time constant of 0.2 s. Spectra A, C, and F were obtained from Act-BLM in *protonated* solvent at g-values of 2.24, 2.16, and 1.97, respectively. Spectrum D was obtained from Act-BLM in *deuterated* solvent at g = 2.16. Spectra B, E, and G were obtained from Fe(III)-BLM in protonated solvent at g-values of 2.38, 2.16, and 1.97, respectively. Spectra A, B, C, E, F, and G took 5 min of signal averaging; D took 10 min.

there was still evidence for strong couplings greater than 10 MHz from both Act-BLM (spectrum 2C) and Fe(III)-BLM (spectrum 2E) although these features were not as well resolved as at g_z. Spectrum 2D provides the ENDOR from a sample of Act-BLM prepared with deuterated solvent to show that the protons having couplings greater than ~5 MHz in spectrum 2C were indeed exchangeable protons. (Similarly, spectra taken at g_z, g_y, or g_x from either Act-BLM or Fe(III)-BLM prepared in deuterated solvent showed that any protons with couplings greater than 5 MHz were exchangeable. Fine detail of non-exchangeable protons having couplings less than 5 MHz was observed with narrow frequency sweeps.) The exchangeable proton features with couplings >10 MHz diminished as the field was moved from g_y toward the minimal g-value g_x (spectra 2F and 2G) and were entirely absent from Act-BLM with couplings >10 MHz at g_x.

Proton ENDOR Discussion. A comparison of our exchangeable proton ENDOR spectra shows that the strongly coupled features have considerable hyperfine anisotropy; the couplings are largest and best resolved at g_z and diminish in intensity and resolution as one goes to g_x. Hyperfine anisotropy is to be expected from protons that can hydrogen bond to nitrogen or oxygen ligands of the metal when their major hyperfine interaction is an anisotropic dipolar interaction.[21] The hyperfine coupling is of the order previously observed for the largest coupling of hydrogen-bonded, exchangeable water protons of

(17) Note that ENDOR spectra obtained at the intermediate g_y value include not only include orientations along the g_y direction but also orientations intersecting the $g_x - g_z$ plane so that they also show the minimal hyperfine coupling as well as the maximal.

(18) Cohen, A. H.; Hoffman, B. M. *J. Phys. Chem.* **1974**, *78*, 1313-1320. See Table I of this reference for an estimate of dipolar coupling ($A_{||}$) to a spin in a 2p oxygen orbital.

(19) Taylor, C. P. S. *Biochim. Biophys. Acta* **1977**, *491*, 137-149.

(20) At g_z, where there is no detectable line broadening, simulations indicate for either the one-oxygen or the two-oxygen model that the hyperfine couplings would have to be larger than 5 G (16 MHz) to be noted; the hyperfine coupling from ENDOR was 7.1 MHz at g_z. The single, narrow ^{17}O feature at g_z also implies either that there is only one contributing ^{17}O or that the hyperfine contributions of two oxygens differ at g_z by less than 3 MHz.

cytochrome P450[6] and of $[VO(H_2O)_5^{2+}]$,[22] where the coupling was along the metal to proton vector and where the bonding to the metal was π bonding. In the P450 case the maximal proton coupling was 10 MHz[6] and in the $[VO(H_2O)_5^{2+}]$ case it was 15 MHz.[22] The majority of the coupling was anisotropic dipolar coupling but with $\sim^1/_3$ arising from isotropic coupling. Estimates of proton metal distances were in the 2.5−2.9-Å range.

A dipolar interaction is largest along the metal-to-proton vector. Here the best defined and largest exchangeable proton couplings were near the g_z direction, and the implication is that there are exchangeable protons attached to ligands along the g_z axis. The g_z direction for low-spin ferric heme has been determined from single-crystal EPR to be perpendicular to the delocalized π-electron heme plane in myoglobin low-spin complexes,[23a,b] in cytochrome c,[23c] and in cytochrome P450.[23d] It has been suggested that the delocalized π-electron system of Fe-BLM provided by pyrimidine conjugated to amide is analogous to the conjugated π-electron heme plane.[3e] The analogy to low-spin ferric heme predicts that the g_z tensor direction of Act-BLM and Fe(III)-BLM ought to be the normal to the π-electron-containing basal plane of bleomycin. The observation of large, well-resolved exchangeable proton features along the g_z direction means that ligands with exchangeable protons are perpendicular to the plane containing the aromatic rings and double bonds. A model which assigns the primary amine and hydrogen-bonding oxygen ligands as axial ligands is consistent with well-resolved, large, exchangeable proton features from protons close to the g_z direction.[24] At g_y where there is still some evidence for strongly coupled exchangeable protons, it is likely that the contribution of exchangeable protons in spectra 2C and 2E arises from in-plane secondary amine protons. The diminution of exchangeable proton intensity near g_x (especially spectrum 2F of Act-BLM) implies that the g_x direction is perpendicular to the vectors from the iron to the exchangeable protons.

(21) Purely dipolar coupling along the metal-to-proton vector is $2g_e\beta_e g_n\beta_n/(R^3h)$, where g_e is the electronic g-value along that vector, β_e and β_n are the respective electronic and nuclear Bohr magnetons, g_n is the nuclear g-value ($g_n = 5.585$) , h is Planck's constant, and R is the distance from metal to proton.

(22) Mustafi, D.; Makinen, M. W. *Inorg. Chem.* **1988**, *27*, 3360−3368.

(23) (a) Helcké, G. A.; Ingram, D. J. E.; Slade, E. F. *Proc. R. Soc. London, Ser. B* **1961**, *169*, 275−288. (b) Hori, H. *Biochim. Biophys. Acta* **1971**, *251*, 227−235. (c) Mailer, C.; Taylor, C. P. S. *Can. J. Biochem.* **1972**, *50*, 1048−1055. (d) Devaney, P. W., Ph.D. Thesis, Electron Spin Resonance of Single Crystals of Cytochrome P450 from Pseudomonas Putida University of Illinois, Urbana, IL, 1980.

(24) Hydrogen-bonded protons of axial oxygen or nitrogen ligands probably do not lie precisely along the metal-to-ligand bond. We performed preliminary angle-selected proton ENDOR simulations using the theory of refs 13a−c and the g-values of Act-BLM. For simulations at a g-value of 2.255 (near but not precisely at g_z), a proton tilted 20° off the g_z axis toward the g_y direction with a dipolar coupling of $A_{||} = 13$ MHz and $A_\perp = -6.5$ MHz yielded ENDOR features with splittings of ~13 and ~7.5 MHz. Such features are consistent with those observed near g_z in Figure 2A.

Conclusions

This Article shows the capability of ENDOR in delineating structure near the iron of bleomycin, especially in its reactive, activated form. Evidence for the nature of the activated oxygen of Act-BLM has been provided. The oxygen is not an oxyferryl oxygen. Its hyperfine coupling shows considerable anisotropy and there is the possibility of resolved quadrupolar coupling. Agreement between ENDOR results and EPR line shape is best if there is only one strongly coupled oxygen. Hyperfine coupling of exchangeable proton features is largest and best resolved along the g_z axis; the implication is that most ligands with exchangeable protons are found along the g_z axis. We suggest that the g_z direction is the direction for ligation of amine and oxygen ligands which can form hydrogen bonds.

This work is a start: more precise elucidation of ^{17}O hyperfine and quadrupolar interactions, elucidation of the differences between proton hyperfine tensors on different ligands for Act-BLM and Fe(III)-BLM, and elucidation of protons potentially involved in O−O bond breaking for Act-BLM and of perturbation by DNA will require numerous ENDOR spectra at different fields and a thorough application of angle-selected ENDOR theory patterned after ref 13.

Acknowledgment. This research was supported in part by NIH Grant No. GM 35103 (to C.P.S.) and American Cancer Society Grant No. CH-443 (to R.M.B.). We are grateful to Prof. Brian M. Hoffman for providing us with his GENDOR simulation routine for our preliminary angle-selected ENDOR simulations.

Supporting Information Available: Figure 1-S contains X-band EPR traces comparing the experimental line shapes at g_x of Act-BLM prepared with $^{16}O_2$ and of Act-BLM prepared with 82.7 atom % $^{17}O_2$ with simulations of the ^{17}O-Act-BLM line shape based on the protocol of the Experimental Section−Methods (2 pages). This material is contained in many libraries on microfiche, immediately follows this article in the microfilm version of the journal, can be ordered from the ACS, and can be downloaded from the Internet; see any current masthead page for ordering information and Internet access instructions.

JA941931B